# A New Alternating Ferro-Antiferromagnetic One-Dimensional Azido-Bridged (Arylazoimidazole)manganese(II), $[Mn(TaiEt)(N_3)_2]_n$ [TaiEt = 1-Ethyl-2-(*p*-tolylazo)imidazole], Exhibiting Bulk Weak Ferromagnetic Long-Range Ordering

**Umasankar Ray,[a] Sk. Jasimuddin,[a] Barindra Kumar Ghosh,[a] Montserrat Monfort,[b] Joan Ribas,*[b] Golam Mostafa,[c] Tian -Huey Lu,[c] and Chittaranjan Sinha*[a]**

**Keywords:** Magnetic properties / Manganese / N ligands / Polymers

1-Ethyl-2-(*p*-tolylazo)imidazole [*p*-Me–$C_6H_4$–N=N–$C_3H_2N_2$–Et-1; TaiEt], an unsymmetrical N,N′-blocker, and azide ($N_3^-$), a versatile intermediary, coordinate to manganese(II) forming an alternating chain with the formula $[Mn(TaiEt)(N_3)_2]_n$ (**1**). The compound crystallizes in the triclinic $P\bar{1}$ space group with $a$ = 7.9297(7) Å, $b$ = 9.5883(9) Å, $c$ = 11.8366(11) Å, α = 103.555(2)°, β = 105.811(2)°, γ = 104.280(2)°, and $Z$ = 2. The structure consists of neutral chains in which each manganese(II) center is alternately bridged by two end-on and two end-to-end azide ligands. The unsymmetrical arylazo heterocycle chelator creates a strong distortion around the metal center [N–Mn–N′ bite 67.7°; Mn–N′(azo) distance 2.562 Å]. The magnetic properties of **1** have been investigated over the temperature range 2–300 K. Magnetic data are analyzed on the basis of an alternating ferro- and antiferromagnetic Heisenberg chain of the manganese(II) ions, described by the spin Hamiltonian $H = -J_1\Sigma S_{2i}S_{2i+1} - J_2\Sigma S_{2i+1}S_{2i+2}$. The $J$ exchange parameters are 2.65 ± 0.12 $cm^{-1}$ and −14.5 ± 0.15 $cm^{-1}$, respectively. Magnetic studies at low temperatures indicate long-range ordering (canting) with a remnant magnetism that vanishes above 40 K. The canting phenomenon has been studied by various techniques including an EPR spectroscopic investigation at different temperatures and appears to be due to the local distortion around each metal center and the π-π stacking in the 3-D network.



## Introduction

The preparation of inorganic-organic hybrid functional materials based on covalent bonds with malleable coordination spheres and non-covalent forces involving hydrogen-bonding X−H···π and π···π interactions is a field of current interest in coordination chemistry.[1−6] Self-assembly[7] is the most efficient approach in this regard. Covalent systems are particularly useful in magnetochemistry as they can provide high magnetic ordering and afford different varieties of magnetic materials.[1,2] A judicious choice of a suitable transition metal template, appropriate organic blocker and efficient magnetic coupler can lead to different molecular architectures with tunable magnetic properties. The pseudohalides, especially azide,[8] are versatile bridging ligands and allow μ-1,1 (end-on, EO), μ-1,3 (end-to-end, EE),[9] μ-1,1,3[10] and other[11,12] modes of interactions. It is established that the μ-1,1 (EO) mode gives ferromagnetic (F) and μ-1,3 (EE) gives antiferromagnetic (AF) interactions[9−12] with few exceptions.[13−16] Different combinations of azide-bridging modes have resulted in some unusual structures which consequently changes the magnetism.[9−30]

To date the maximum number of reports on azide-bridging coordination polymers with various organic blockers and investigations of their structure and magnetism have appeared for copper(II) and nickel(II).[9−21] In this regard, analogues studies of other 3d ions like manganese, iron, cobalt are less familiar. The manganese−azido system is currently attracting the attention of magnetochemists, since it enables work to be done with a greater local spin value.[9] The use of different heterocyclic N-donor ligands such as pyridine, polypyridine and their substituted derivatives, pyridine Schiff bases, are well documented.[9,22−30] But no such work has been initiated with unsymmetrical ligands having azo-N and heterocyclic-N donor centers. Arylazo heterocycles with the azoimine (−N=N−C=N−) function are unsymmetrical *N*,*N*′-end-capping chelators. For the last few years our group has been engaged[31−34] in exploring

[a] Department of Chemistry, The University of Burdwan, Burdwan 713104, India
E-mail: c_r_sinha@yahoo.com
[b] Departament de Quimica Inorganica, Universitat de Barcelona, Diagonal 647, 08028 Barcelona, Spain
E-mail: joan.ribas@qi.ub.es
[c] Department of Physics, National Tsing Hua University, Hsinchu 30043, Taiwan, ROC

  DOI: 10.1002/ejic.200300415 

the chemistry of such ligand systems with transition and non-transition metal ions. Ligands have been anchored on a surface to synthesize a solid-phase extractant[34] that has been used in the separation of different $d^n$ ions from ores, alloys, medicinal samples, etc.

With this background we are interested in preparing and characterizing new polynuclear azidomanganese(II) complexes with a bidentate azoimidazole ligand, 1-ethyl-2-(*p*-tolylazo)imidazole (TaiEt). The ligand system plays a substantial role in chemistry[31−33] involving stabilizing low oxidation states of transition metal ions. We have used metal/bidentate ligands in 1:1 ratios in such a way that the four coordination vacancies around the six-coordinate manganese(II) ion should be completed by the excess azide ligands. According to this principle, we are able to prepare a new alternating double-bridged μ-1,1 (EO) and μ-1,3 (EE) azidomanganese(II) complex of TaiEt with a one-dimensional (1-D) chain along with noncovalent C−H···π and *p*···π inter-chain interactions leading to a 3-D geometry, which has been characterized by X-ray diffraction and spectroscopic studies. Magnetic measurements indicate global AF behavior with the presence of a weak F component intrinsic to the sample. The most interesting feature is the weak long-range ferromagnetic ordering likely to occur due to a canting phenomenon originating from the local distortion around the manganese(II) centers and the π-π stacking in the 3-D network.

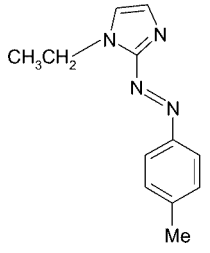


## Results and Discussion

### Synthesis and Formulation

The preparation of **1** can be achieved in high yield by the reaction of $Mn(OAc)_2{\cdot}4H_2O$ with TaiEt and $NaN_3$ in dry MeOH at room temperature. The procedure is summarized in Equation (1).

The organic blocker belongs to the unsymmetrical *N*,*N*′-chelating ligand, where N and N′ are the N(imidazole) and N(azo) donor centers, respectively. The air-stable moisture-insensitive red-brown compound is insoluble in common organic solvents. In the IR spectrum the asymmetrical azido stretch, $\nu_{assym}(N_3)$ appears as strong bands between 2095 and 2050 $cm^{-1}$ which suggests the simultaneous existence of EE and EO bridging modes in the complex.[9,35] The azide symmetric stretch $\nu_{sym}(N_3)$ corresponding to the EO bridging mode can be observed as a band of medium intensity at 1330 $cm^{-1}$. This mode is not active for the symmetrical EE coordination. Finally, the band assignable to the deformation mode of the azido group, $\delta(N_3)$, found at 610, 600 $cm^{-1}$, is in good agreement with that observed for all polynuclear azido compounds.[9,35] Furthermore, the pertinent bands characteristic of the bound TaiEt ligand appear at 1590 [ν(C=N)] and 1395 [ν(N=N)] $cm^{-1}$. The diffused reflectance spectrum of $[Mn(TaiEt)(N_3)_2]_n$ exhibits an intraligand charge transfer transition at 380 nm and weak spin-forbidden *d*-*d* bands at 525 (sh) and 455 nm corresponding to an octahedral symmetry.[36]

### Description of the Structure

The structure of $[Mn(TaiEt)(N_3)_2]_n$ was revealed by a single-crystal X-ray diffraction study [Figure 1, (a) and (b)]. Selected bond lengths and angles are given in Table 1. Each manganese center exhibits a distorted octahedral $MnN_6$ coordination sphere linked by two EO and two EE azide groups as well as two N-centers from *N*,*N*′-chelator (TaiEt), respectively, forming four-membered, eight-membered and five-membered loops around each metal center. The chelate angle =N−Mn−N′ is 67.7(1)° which is smaller than those reported values for other transition metal arylazo complexes[31−33,37,38] [76.5° for a ruthenium(II) complex[37] and 77.8° for an osmium(II) compound].[38] This may have a major influence on distortion from idealized $O_h$ symmetry. The Mn−N(azo) bond [Mn−N(1), 2.562(2) Å] is elongated by 0.34 Å compared to the Mn−N(imidazole) distance [Mn−N(3), 2.221(2) Å]; however, it is well below the sum of the van der Waals radii of $Mn^{II}$ and N(azo).[39] The N=N bond [N(1)−N(2), 1.267(3) Å] is longer than that of the free ligand [1.252(1) Å].[40] This increment may refer to a dπ(Mn)→π*(azo) charge transition.[32]

The atomic arrangements Mn, N1, N2, C8, N3 constitute a plane (mean deviation < 0.07 Å) and the pendant phenyl ring makes a dihedral 16.83(2)° with the plane. The manganese(II) ions are alternately linked by two EO [Mn−N(8) 2.217(2) Å, Mn−N(8a) 2.214(3) Å] and two EE [Mn−N(5) 2.204(3) Å, Mn−N(7b) 2.215(3) Å] azido bridges. The Mn−N(8)−Mn(a) angle in the EO mode is 103.53(9)° and lies within the range (100−105°)[9] for this kind of bridge. The bridging arrangement Mn−N(8)−Mn(a)−N(8a) is planar but the azide ligands do not reside within the plane. The Mn−N(5)−N(6) and Mn−N(7b)−N(6b) angles are 135.3(2)° and 130.1(2)°, respectively. The dihedral angle between the mean plane of Mn−N(5)−N(6)−N(7) and Mn−N(7b)−N(6b)−N(5b) with a chair configuration is 3.5°. The dihedral angle between the least-squares plane formed by the six N atoms of the EE double-bridging azide ligands and the N(5)−Mn−N(7b) system is 1.82(13)°. The

$$n\ Mn(OAc)_2{\cdot}4H_2O + n\ TaiEt + 2n\ NaN_3 \xrightarrow[25°C]{MeOH} [Mn(TaiEt)(N_3)_2]_n + 2n\ NaOAc + 4n\ H_2O \quad (1)$$

  

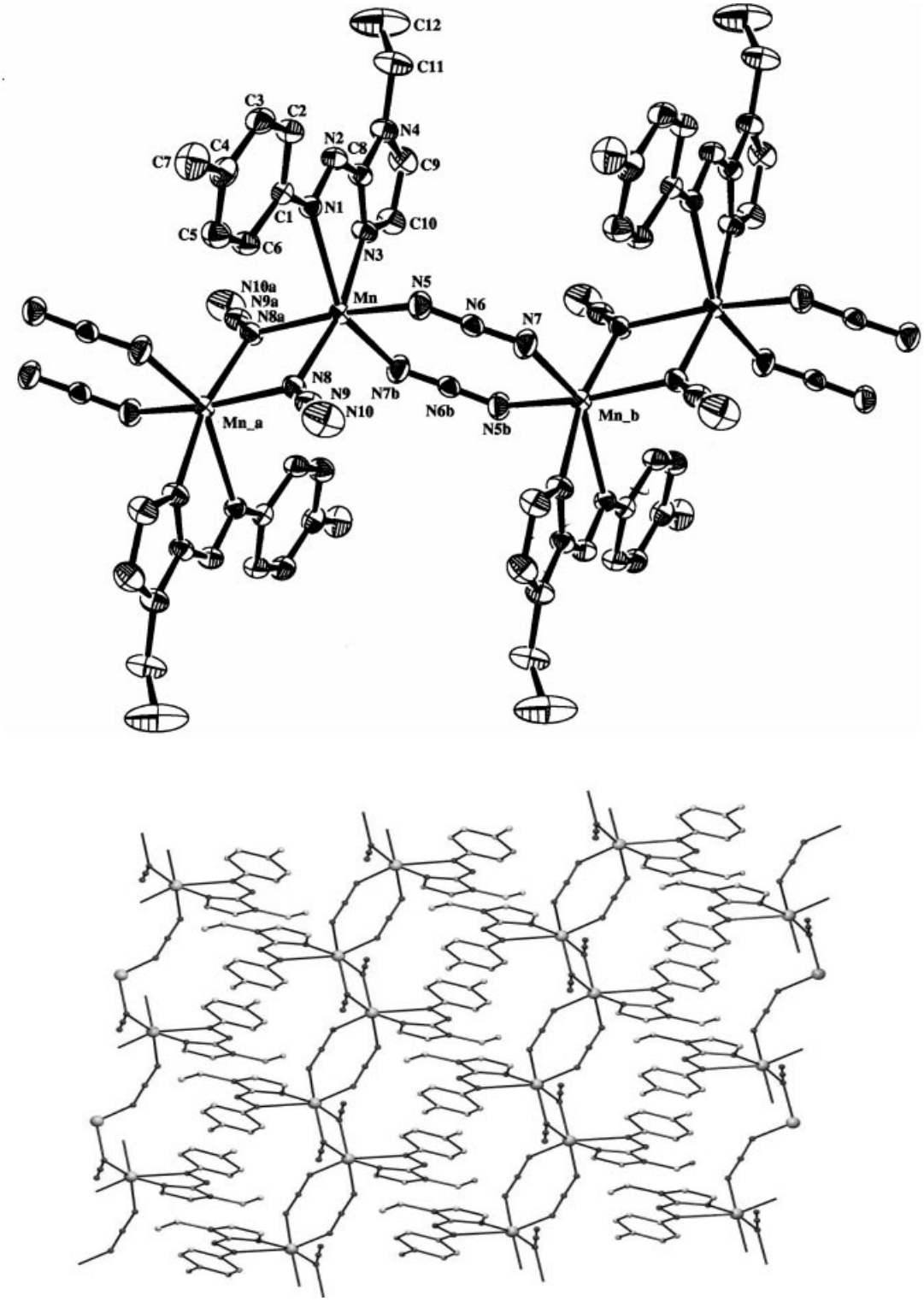


Figure1. (a; top) ORTEP view of the enchainment in $[Mn(TaiEt)(N_3)_2]_n$ with atom numbering scheme; (b; bottom) section of the packing arrangement due to noncovalent interactions of $[Mn(TaiEt)(N_3)_2]_n$ (**1**)

N−N distances of the azide ligand ranges from 1.144(4) to 1.194(3) Å and reflects typical double-bond character. In the EO mode, the N−N distance of terminal and bridging types exhibit usual distortion (ca. 0.05 Å) compared to the symmetrical bond lengths in the EE motif; but the results show that in the EE motif the azide ligand is slightly distorted from linearity [N(5)−N(6)−N(7) 177.1(3)°] compared to the EO azide form [N(8)−N(9)−N(10) 179.4(4)°]. One [N(5)] of the EE azide N atom is *trans* with that of the EO azide N atom [N(8a)] and the mutual inclination is

  

Table 1. Selected bond lengths [Å] and angles [°] for **1**

| | | | |
|---|---|---|---|
| Mn−N(1) | 2.562(2) | Mn−N(3) | 2.221(2) |
| Mn−N(5) | 2.204(3) | Mn−N(8) | 2.217(2) |
| Mn−N(8a) | 2.214(3) | Mn−N(7b) | 2.215(3) |
| N(1)−N(2) | 1.267(3) | N(2)−C(8) | 1.386(3) |
| N(5)−N(6) | 1.162(4) | N(6)−N(7) | 1.164(4) |
| N(8)−N(9) | 1.194(3) | N(9)−N(10) | 1.144(4) |
| Mn−Mn a | 3.461 | Mn−Mn b | 5.400 |
| N(3)−Mn−N(5) | 97.59(9 | N(3)−Mn−N(8) | 167.22(10) |
| N(3)−Mn−N(7b) | 87.46(10) | N(3)−Mn−N(8a) | 95.86(9) |
| N(3)−Mn−N(1) | 67.75(7) | N(5)−Mn−N(8a) | 165.16(9) |
| N(5)−Mn−N(7b) | 91.72(11) | N(5)−Mn−N(1) | 79.61(9) |
| N(5)−Mn−N8 | 89.15(9) | N(8)−Mn−N(8a) | 76.47(9) |
| N(8)−Mn−N(7b) | 103.25(11) | N(8a)−Mn−N(7b) | 95.11(11) |
| Mn−N(3)−C(8) | 116.29(16) | N(1)−N(2)−C(8) | 112.3(2) |
| Mn−N(5)−N(6) | 135.3(2) | N(5)−N(6)−N(7) | 177.1(3) |
| Mn(b)−N(7)−N(6) | 130.1(2) | Mn−N(8)−N(9) | 127.0(2) |
| Mn−N(8)−Mn(a) | 103.53(9) | Mn(a)−N(8)−N(9) | 128.0(2) |
| N(8)−N(9)−N(10) | 179.4(4) | | |

| Non-covalent interactions: C−H···π/π···π (coordinates) | H···$C_g$/$C_g$···$C_g$ [Å] | Dihedral angle [°] |
|---|---|---|
| C(7)−H(7C)···$C_g$(1) (−$x$, 1 − $y$, 1 − $z$) | 2.758(4) | 146.20 |
| C(11)−H(11b)···$C_g$(2) (1 − $x$, 1 − $y$, 1 − $z$) | 2.707(3) | 143.90 |
| $C_g$(1)···$C_g$(1) (−$x$, −$y$, 1 − $z$) | 3.416(2) | 0.03 |
| $C_g$(1)···$C_g$(2) (−$x$, 1 − $y$, 1 − z) | 3.525(2) | 12.60 |
| $C_g$(2)···$C_g$(1) (1 − $x$, 1 − $y$, 1 − $z$) | 3.136(2) | 12.60 |
| $C_g$(2)···$C_g$(2) (−$x$, 1 − $y$, 1 − $z$) | 3.545(2) | 0.00 |
| $C_g$(1): N(3)−C(8)−N(4)−C(9)−C(10) | | |
| $C_g$(2): C(1)−C(2)−C(3)−C(4)−C(5)−C(6) | | |

165.16(9)°. The imidazole N center [N(3)] of TaiEt is *trans* to the EO azide N atom [N(8)] while the azo N atom [N(1)] is *trans* to the EE azide N atom [N(7b)]. This reveals a 1-D chain structure of the molecule, which is being supported by EO and EE Mn−$N_3$ motifs.

The C−H···π and π···π interactions are two noncovalent forces operating among the molecules to generate a three-dimensional network.[41−43] Each molecular unit shows two C−H···π bonding interactions [C(7)−H(7C)···$C_g$(1) and C(11)−H(11b)···$C_g$(2)] with imidazole [$C_g$(1)] (−$x$, 1 − $y$, 1 − $z$) and *p*-tolyl [$C_g$(2)] (1 − $x$, 1 − $y$, 1 − $z$) rings of neighboring molecules [Table 1, Figure 1 (b)]. The C(7)−H(7c) bond is from the methyl group of ($C_6H_4$)−$CH_3$ (*p*), and C(11)−H(11b) is part of the methylene moiety of the N(4)−$CH_2$−($CH_3$) group. Their interactions with $C_g$(1) and $C_g$(2), respectively, may provide inter-chain rigidity and is the operating force of a 3-D network. The *p*···π interactions $C_g$(1)···$C_g$(1) [3.416(2) Å], $C_g$(1)···$C_g$ (2) [3.525(2) Å], $C_g$(1)···$C_g$(2) [3.136(2) Å] and $C_g$(2)···$C_g$(2) [3.545(2) Å] enhance the inter-chain networking strength. These noncovalent interactions among 1-D parallel units are ideal in forming a 3-D supramolecular continuum.

## Magnetic Properties

The temperature dependence of the magnetic susceptibility is shown in Figure 2. The $\chi_M$ value is 0.0123 $cm^3 \cdot mol^{-1}$ at 300 K and increases smoothly with decreasing

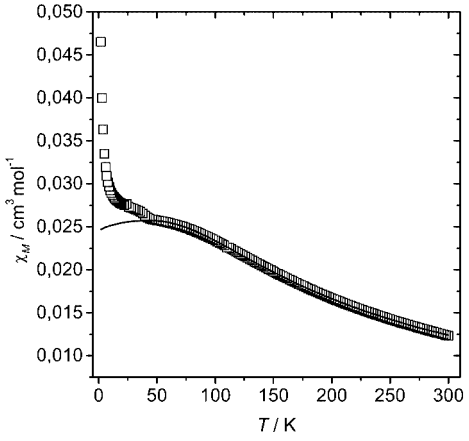


Figure 2. Plots of $\chi_M$ vs. $T$ for **1**; the solid line represents the best fit (see text for the parameters calculated)

temperature (0.025 $cm^3 \cdot mol^{-1}$ at 50 K), and finally increases abruptly to a maximum value of 0.0465 $cm^3 \cdot mol^{-1}$ at 1.95 K. This reflects global antiferromagnetic coupling with the presence of a weak ferromagnetic long-range ordering down to 40 K presumably due to a canting phenomenon.[44] Thus, unusual $\chi_M$ values at low temperatures restrict us in fitting all of the magnetic data: it is only possible to fit the data to the temperature where the canting arises (40 K) (see below). To avoid any misleading interpretation we have carried out the fitting from 300−50 K.

  

**(a) High-Temperature Zone (300−50 K) − Calculation of the Coupling Parameters**

The structural findings demand an alternating chain of exchange interactions with nearest neighbors that have been described by the spin Hamiltonian where $J_1$ and $J_2$ stand for the alternating exchange constants, and "classical" spin operators are expressed by $S$ are.

$$H = -J_1\Sigma S_{2i}S_{2i+1} - J_2\Sigma S_{2i+1}S_{2i+2}$$

This approximation is justified for manganese(II) ion, which exhibits a large spin ($S = 5/2$). The fit of experimental data for such a manganese(II) 1-D system has been carried out using the reported relation[26] derived from the above Hamiltonian, in Equation (2), in which $u_1 = \coth(J_1/kT) - kT/J_1$, $u_2 = \coth(J_2/kT) - kT/J_2$ with the scaling factors $J_i = J_{i'}S(S + 1)$ and $g_i = g_{i'}[S(S + 1)]^{1/2}$.[26]

$$\chi = \frac{Ng^2\beta^2}{3kT}\left(\frac{1+u_1+u_2+u_1u_2}{1-u_1u_2}\right) \quad (2)$$

The best $J$ parameters obtained are: $2.7 \pm 0.10$ cm$^{-1}$ and $-14.6 \pm 0.15$ cm$^{-1}$, $g = 2.01$ and $R = 2.56 \times 10^{-9}$. If $g$ is kept at 2.00, which is the expected value for $Mn^{II}$, $J_1$ and $J_2$ do not differ significantly: $2.65 \pm 0.12$ cm$^{-1}$ and $-14.5 \pm 0.15$ cm$^{-1}$ and $R = 1.75 \times 10^{-8}$. A negative $J$ value (AF) can be attributed to the EE azido bridge whereas the positive $J$ value (F) corresponds to the EO mode.[9] The main structural and magnetic parameters of the reported alternating manganese(II) 1-D azido systems along with **1** are collected in Table 2 for a comparison of the magnetic behavior. Assuming that the Mn−N distances do not vary considerably, the main factor controlling the intensity of the ferromagnetic interactions in the EO bridge appears to be the bridging Mn−N(azido)−Mn angle (θ). Density functional calculations[45,46] on some model compounds of manganese(II) show a parabolic dependence of $J$ on this bridging angle (θ): for θ lower than 98°, AF coupling is expected; for θ greater than 98°, F coupling should result.[45] A crossover from F to AF is predicted at θ = 98°. The angles (see Table 2) are close to 100° and $J$ values vary from 9.6 to 1.8 cm$^{-1}$. **1** has a very large angle (θ = 103.5°); thus, its $J$ value should be one of the largest. However, it is one of the lowest $J$ values (2.65 cm$^{-1}$) indicating that the correlation of $J$ with θ may be complicated and a more accurate pragmatic theory is needed to systematize this behavior.

Now assuming that the Mn−N distances do not vary considerably, the most useful structural parameter for examining the magnitude of the AF coupling via EE bridges

Table 2. Main magnetostructural parameters for alternating EE−EO one-dimensional Mn−azido systems [3-bzpy = 3-benzoylpyridine; 3-Et,4-Mepy = 3-ethyl-4-methylpyridine; bpy = 2,2′-bipyridine; bpm = bis(pyrazol-1-yl)methane; dpa = 2,2′-dipyridylamine; 3-ampy = 3-aminopyridine; $L^1$ = *N*-phenyl-2-carbaldimine; $L^2$ = *N*-(*p*-tolyl)-2-carbaldimine; $L^3$ = *N*-(*m*-tolyl)-2-carbaldimine; $L^4$ = *N*-(*p*-chlorophenyl)-2-carbaldimine; $L^5$ = *N*-(*m*-chlorophenyl)-2-carbaldimine; TaiEt = 1-ethyl-2-(*p*-tolylazo)imidazole)]

| Complex | θ[a] [°] | δ[b] [°] | *J* (*ferro*) [cm$^{-1}$] | *J* (*antiferro*) [cm$^{-1}$] | Ref. |
|---|---|---|---|---|---|
| Double EE/double EO *trans* geometry of non-azido ligands | | | | | |
| $[Mn(3\text{-bzpy})_2(N_3)_2]_n$ | 100.4 | 26.6 | 3.5 | −12.3 | [22] |
| $[Mn(3\text{-Et,4-Mepy})_2(N_3)_2]_n$ | 99.7 | 31.7 | 2.4 | −13.7 | [23] |
| Double EE/double EO *cis* geometry of non-azido ligands | | | | | |
| $[Mn(bpy)(N_3)_2]_n$ | 101.0 | 22.7 | 9.6 | −11.9 | [26] |
| $[Mn(bpm)(N_3)_2]_n$ | 102.9 | 20.5 | 15.7 (**1.80**)[c] | −63.7(−**7.28**)[c] | [27] |
| $[Mn(dpa)(N_3)_2]_n$ | 102.9 | 35.1 | 45 (**5.14**)[c] | −53 (−**6.05**)[c] | [24] |
| $[Mn(L^1)(N_3)_2]_n$ | 99.6 | 9.8 | 3.8 | −15.4 | [25] |
| $[Mn(L^2)(N_3)_2]_n$ | 101.6 | – | 5.2 | −11.8 | [25] |
| $[Mn(L^3)(N_3)_2]_n$ | 103.9 | 19.5 | 7.2 | −13.7 | [25] |
| $[Mn(L^4)(N_3)_2]_n$ | 100.6 | 9.8 | 4.1 | −13.3 | [25] |
| $[Mn(L^5)(N_3)_2]_n$ | 104.0 | 12.0 | 8.0 | −14.4 | [25] |
| $[Mn(TaiEt)(N_3)_2]_n$ | 103.5 | 1.82 | 2.65 (12) | −14.5 (15) | this work |
| Single EE/double EO | | | | | |
| $[Mn(3\text{-Et,4-Mepy})_3(N_3)_{1/2}](PF_6)$ | 101.4 | – | 3.3 | −5.2 | [28] |
| $[Mn(3\text{-ampy})_2(N_3)(H_2O)]_n$ | 99.6 | – | 2.3 | −6.0 | [28] |

[a] θ corresponds to the Mn−N(azido)−Mn angle. [b] δ is defined in Scheme 1. [c] The $J$ values reported in refs.[24,27] have been simulated by us because they seemed to be too large. Effectively, the simulation using the same formula indicated in the text (ref.[26]) does not agree at all with the figures of $\chi_M$ vs. $T$. On the contrary, dividing by $S(S + 1) = 5/2 \times 7/2 = 8.75$ the recalculated $J$ values (indicated in parentheses in bold) perfectly agree with the figures given in refs.[24,27] This error may be due to the meaning of $J$ given in ref.[24]; the scaling factor is $J_i = J_{i'}S(S + 1)$ used by us, which has not been used in these two papers.

  

is the dihedral angle (δ) (Scheme 1). EHMO calculations[24,26] show that the AF coupling should decrease for larger values indicating that the loss of overlap due to the increase in the torsion angle becomes the driving parameter controlling the magnitude of the exchange interaction. For **1**, the δ value is the lowest reported so far (1.82°) (Table 2). Thus, the AF coupling should be greater. In fact, it is the highest $|J|$ value (14.5 $cm^{-1}$) reported to date. At this stage it is very difficult to draw a general conclusion. Other complexes with high δ values (close to 30°, for example, in the two complexes[22,23] with a *trans* blocker) have similar $J$ values (Table 2) when, theoretically, this should be very small. So new compounds and more accurate calculations are necessary to systematize these kinds of magnetostructural correlations in the manganese(II) systems.

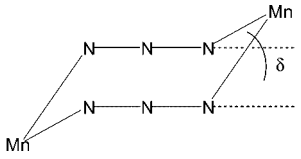


Scheme 1

### (b) Low-Temperature Zone (50−2 K) − Origin of the Weak Ferromagnetism

The increase in susceptibility down to ca. 45−50 K indicates the presence of a weak intrinsic ferromagnetic contribution, possibly due to a spin canting effect.[44] A cursory report of a similar feature is found in only one of the alternating EE and EO azido-bridged 1-D manganese complexes (Table 2).[24] In the present case, extensive experiments have been performed to substantiate the long-range ordering as pointed below.

(1) An abrupt break in $\chi_M$ and $\chi_M T$ occurs at 40 K when lower fields are employed (Figure 3). This transition at 40 K, when the magnetic field changes, is indicative of the onset of long-range magnetic ordering.[47]

(2) The field-cooled magnetization (FCM) obtained on cooling within the field (50 Oe) shows the typical feature [Figure 4 (a)] of a ferromagnetic transition, i.e. a rapid increase in $\chi_M$ occurs when $T$ decreases below 40 K and, then, appears at the beginning of saturation. If the field is switched off below 40 K, a remnant magnetization is observed. The zero-field-cooled magnetization (ZFCM) is obtained by cooling in zero-field and then applying the field and heating. At any temperature below $T_c$ the ZFCM is smaller than the FCM, due to the fact that in this temperature range the applied field is too weak to move the domain walls. The remnant magnetization (RM) [Figure 4 (b)] indicates the presence of magnetization from 2 to 40 K. Thus, the critical temperature for the long-range magnetic ordering is 40 K.

(3) The magnetization study (from −5 T to +5 T at 2 K) shows (Figure 5) the $M/N\beta$ value to be 0.3 $e^-$, which is clearly indicative of the global antiferromagnetic interaction. An isolated manganese(II) ion would give 5 $e^-$. At the

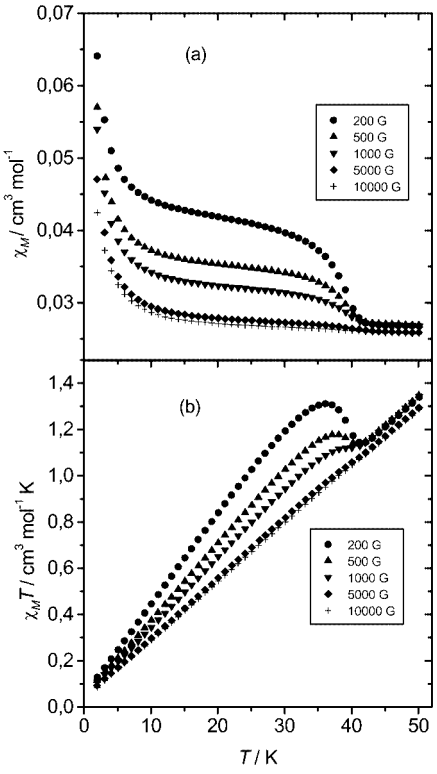


Figure 3. Plots of (a) $\chi_M$ vs. $T$ and (b) $\chi_M T$ vs. $T$ at different fields in the temperature range (2−50 K); at lower fields abrupt breaks are seen (see text)

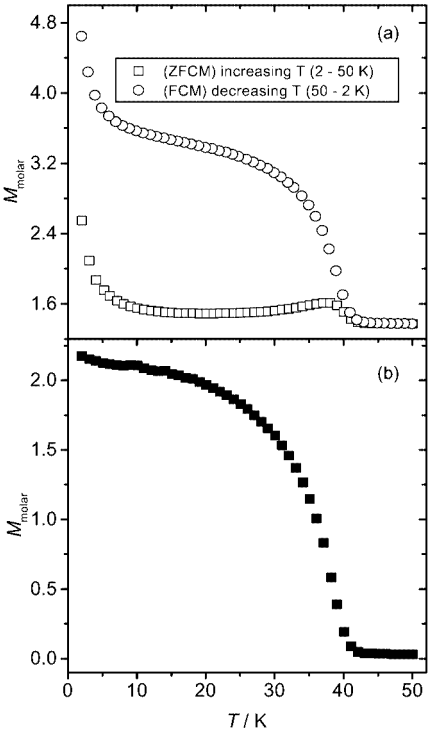


Figure 4. (a) Field-cooled magnetization (FCM) and zero-field-cooled magnetization (ZFCM) for **1**; (b) remnant magnetization as a difference of FCM and ZFCM, from 50−2 K

  

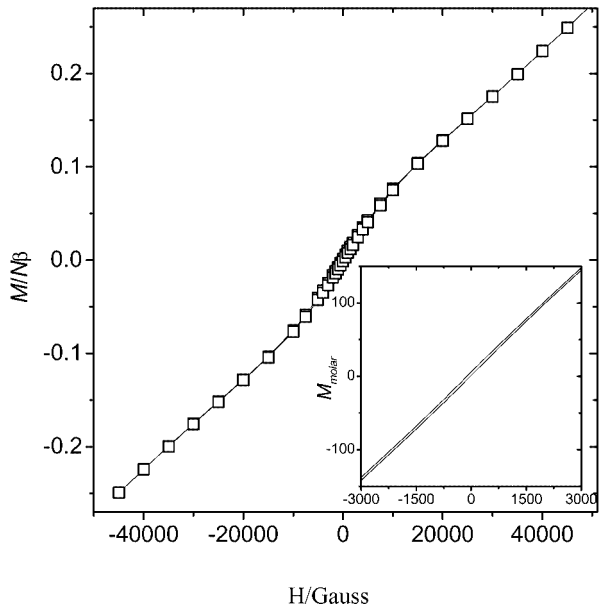


Figure 5. Reduced magnetization curve for **1**, at 2 K; (inset) central part of the magnetization curve for **1**, showing a very small hysteresis loop

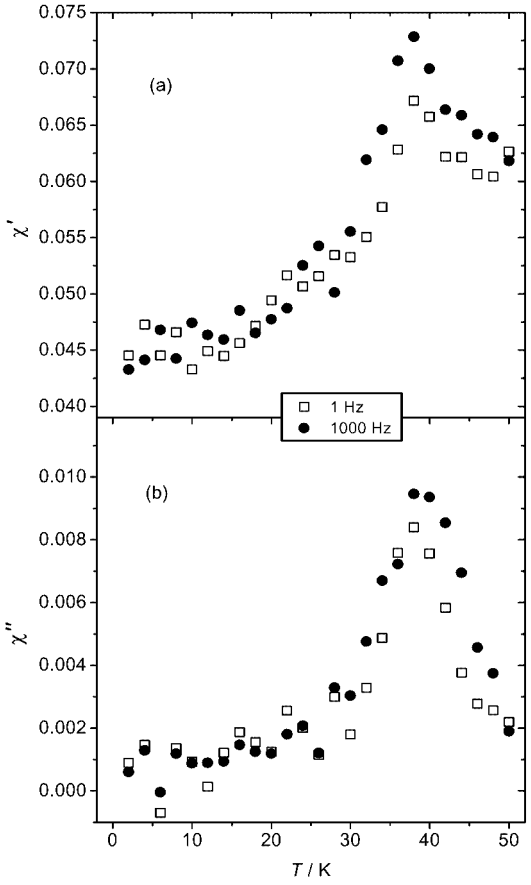


Figure 6. *In-phase* (a) and *out-of-phase* (imaginary) (b) parts of the *ac* susceptibility curves for **1** at two different frequencies (1 and 1000 Hertz)

bottom of the figure (from −0.5 T to +0.5 T) a weak hysteresis loop is seen. The coercive field is difficult to calculate, as it is too large, but the remnant magnetization at 0 K is 6.7 $cm^3$ Gauss·$mol^{-1}$, which is typical of a soft ferromagnet.

(4) The *ac* susceptibility measurements are definitely the best proof of the long-range order. The real part of the *ac* magnetic susceptibility ($\chi_{ac}'$) has a maximum at ca. 40 K, accompanied by the occurrence of non-zero field-independent $\chi_{ac}''$ (Figure 6) suggesting that the $T_c$ of **1** is close to 40 K. The small $\chi$ values indicate weak ferromagnetic character (in accordance with the hysteresis loop values).

(5) EPR spectroscopic measurements at room temperature (298 K) show a very intense isotropic signal centered at $g = 2.00$ (without hyperfine splitting) which is typical for the manganese(II) ion. The peak-to-peak band-width increases on lowering the temperature (at 298 K and 77 K it is ca. 150 Gauss; at 40 K it is ca. 400 Gauss) (Figure 7) and its intensity strongly diminishes. Finally, at 4 K the peak-to-peak band-width is > 2000 Gauss and 1600 times less intense than that at room temperature, which is in accordance with the behavior of long-range ordered compounds at low temperature.[48] It is worth mentioning that this feature in the EPR spectra indicates that the magnetic ordering cannot be attributed to ferromagnetic impurities and the canting phenomenon must be inherent to the sample. Canted one-dimensional (1-D)[49−51] and/or discrete[52] systems are reported in the literature though very scarce. Instead, canting is more frequent in two-dimensional (2-D) and three-dimensional (3-D) systems[53] because the canting, per se, is a three-dimensional long-range ordering. To interpret this behavior in 1-D, it is necessary to have some linkages in **1**, though weak, resulting in a 3-D network. This may be attributed to the π···π stacking (Figure 1, b) and other weak interactions. The spin canted structure is *not compatible* with the crystal structure of **1** because of the presence of an inversion center (space group $P\bar{1}$). Thus, the existence of the possible canting effect must be due to a distortion in the crystal net at low temperatures, that suppresses the inversion center. It is well known that two mechanisms lead to spin canting: (i) magnetic anisotropy ($D$ and $E$) and (ii) antisymmetric exchange, $\boldsymbol{d}_{ij}[S_i \times S_j]$.[44,54] In both cases, the total energy is minimized through a compromise in which the spins are tilted away from the antiparallel towards a position in which they are perpendicular (Scheme 2). The $D$ parameter is, in principle, non-zero because the ground state is $S = 5/2$ and there is a great distortion in the manganese(II) ion as is evident from the N−Mn−N′ angle of 67.7° created by the chelator and from lengthening of the Mn−N(azo) bond (2.56 Å) over the other five Mn−N bonds (ca. 2.2 Å). The Mn−N(azo) distance is anomalously long creating greater distortion and anisotropy. Such a coordination environment plays a major role for the canting behavior in this case and as also found in some manganese(III)[55,56] ($S = 2$) and nickel(II)[50,57] ($S = 1$) systems. The other possible origin of the canting, the antisymmetric part of the spin Hamiltonian, is proportional to $[(g - 2)/g]J$, where the intermolecular coupling, $J$ is an average between −14.5 and 2.65 $cm^{-1}$. The average $g$ value

  

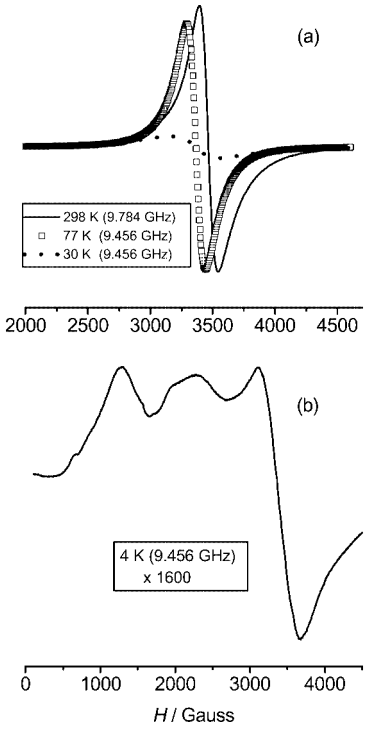


Figure 7. EPR spectra of powder sample of **1** (a) at 298 K, 77 K and 30 K with the same scale; (b) the spectrum a 4 K with a very large scale (see text)

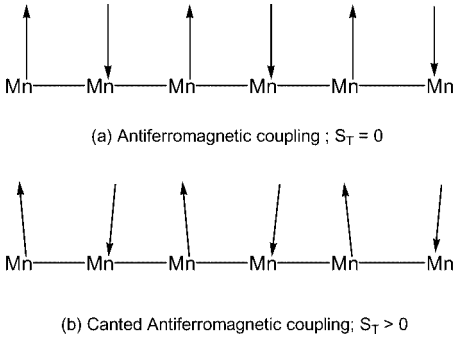


Scheme 2

is close to 2.00. Thus, although very small, this term could not be nullified. Such an explanation is found in the literature for several non-distorted iron(III),[58] manganese(II)[59,60] and copper(II) canted complexes.[61,62] In the present case, the magnetization curve allows us to calculate the (possible) canting angle. According to the literature, there are several approaches to calculate the canting angle.[22,44] The most useful is $\sin^{-1}(\mu_{RM}/\mu_{satd.})$ or $\sin^{-1}(M_{RM}/M_{satd.})$ being $\mu_{sat} = 5$ for manganese(II) ions. In complex **1**, $M_{RM}$ is 0.3, thus the angle is very small (0.34°) and results in a very small ferromagnetic ordering.

## Conclusion

We have presented here the synthesis, single-crystal X-ray structure, and magneto-structural correlation of a new 1-D azido-bridged manganese(II) coordination polymer. The structural characterization shows an alternating bis(-bridged) EE and EO azido network with a very unsymmetrical organic blocker as a *cis* chelate. The presence of C−H···π and π···π interactions leads to the generation of a three-dimensional network. From the magnetic point of view the complex shows a long-range magnetic order arising due to a canting phenomenon originated most likely from the distortion created by the low bite of the chelator resulting a very strong distortion in the Mn−N(azo) distance (2.56 Å) and 3-D structural evolution. The use of an arylazo heterocycle ligand system over pyridine or polypyridine systems[22−30] provides ample scope for such long-range magnetic ordering. We are currently working with this azo heterocycle having varied substituents on its network to prepare different molecular architectures with other 3d transition metal ions using pseudohalide intermediaries and to study their magnetic behavior towards the preparation of molecule-based magnets.

## Experimental Section

**Materials:** Manganese(II) acetate tetrahydrate (SRL, India) and sodium azide (SRL, India) were purchased and used without further purification. 1-Ethyl-2-(*p*-tolylazo)imidazole (TaiEt) was prepared according to a reported procedure.[31] All other chemicals and solvents for preparative and spectroscopic work were of reagent grade and were used as received.

***CAUTION!*** Azido complexes of transition metal ions containing organic ligands are potentially explosive. Only a small amount of material should be prepared, and it should be handled with care.

**Physical Measurements:** IR spectra (KBr discs, 4000−300 $cm^{-1}$) were recorded with a JASCO FTIR model 420 spectrophotometer. Microanalyses (C, H and N) were done with a Perkin−Elmer 2400 CHNS/O elemental analyzer. The diffuse reflectance spectrum was run at room temperature with a JASCO UV/Vis/NIR V-570 spectrophotometer in the 200−1000 nm range. A Bruker ES 200 spectrometer (X-band frequency) was used to record the EPR of polycrystalline samples at room (298 K) and low temperatures (77 K, 30 K, 4 K). Magnetic measurements on powdered samples were performed over the temperature range 2−300 K using a Quantum Design MPMS-7 SQUID magnetometer in a magnetic field of 0.1 T. The experimental susceptibilities were corrected for the diamagnetism of the constituent atoms (Pascal tables).

**Synthesis of the Complex $[Mn(TaiEt)(N_3)_2]_n$ (1): 1** was synthesized from $Mn(OAc)_2{\cdot}4H_2O$ (0.100 g, 0.408 mmol), TaiEt (0.087 g, 0.408 mmol) and $NaN_3$ (0.053 g, 0.816 mmol) in dry methanol solution (25 mL). The resulting intense red solution was filtered and left to stand at room temperature. After several days, prismatic dark-red single crystals were obtained. They were separated by filtration, washed with $Et_2O$ and dried in vacuo over indicator silica gel. Yield: 0.124 g (75%). $C_{12}H_{14}MnN_{10}$ (353.27): calcd. C 40.8, H 4.0, N 39.7; found C 40.6, H 3.9, N 39.5.

  

**X-ray Structure Determination:** A suitable single crystal of the title complex for X-ray analysis was mounted on a Siemens SMART CCD diffractometer equipped with a graphite monochromator and Mo-$K_\alpha$ ($\lambda$ = 0.71073 Å) radiation. Data were collected at 295 K. The crystal size was 0.08 × 0.10 × 0.18 mm. The intensity data were corrected for Lorentz and polarization effects and an empirical absorption correction was also employed using the SAINT[63] program. A summary of the crystallographic data and structure refinement parameters is given in Table 3. A total of 7947 reflections (unique reflections, 3546, $R_{int}$ = 0.029) were collected in the range 1.9° < θ < 28.1° and 2683 were assumed applying the condition $I > 2\sigma(I)$. The structure was solved by the Patterson method using SHELXS-97[64] followed by Fourier and difference Fourier synthesis. Full-matrix least-squares refinements on $F^2$ were carried out using SHELXL-97 with anisotropic displacement parameters for all non-hydrogen atoms. The hydrogen atoms were fixed geometrically and refined using a riding model. In the final difference Fourier map the residual maxima and minima were 0.52 and −0.38 e·Å$^{-3}$. All calculations were carried out using the SHELXL-97, ORTEP-32[65], PLATON[66] programs. CCDC-193975 contains the supplementary crystallographic data for this paper. These data can be obtained free of charge at www.ccdc.cam.ac.uk/conts/retrieving.html [or from the Cambridge Crystallographic Data Centre, 12 Union Road, Cambridge CB2 1EZ, UK; Fax: (internat.) + 44-1223/336-033; E-mail: deposit@ccdc.cam.ac.uk].

Table 3. Crystal data and details of the structure determination for **1**

| | |
|---|---|
| Empirical formula | $C_{12}H_{14}MnN_{10}$ |
| Formula mass | 353.27 |
| Temperature [K] | 295 |
| Radiation λ [Å] | 0.71073 |
| Crystal system | triclinic |
| Space group | $P\bar{1}$ |
| *a* [Å] | 7.9297(7) |
| *b* [Å] | 9.5883(9) |
| *c* [Å] | 11.8366(11) |
| α [°] | 103.555(2) |
| β [°] | 105.811(2) |
| γ [°] | 104.280(2) |
| *V* [Å$^3$] | 794.05(13) |
| *Z* | 2 |
| $d_{calcd.}$ [g·cm$^{-3}$] | 1.478 |
| μ [mm$^{-1}$] | 0.847 |
| *F*(000) | 362 |
| Crystal size [mm] | 0.08 × 0.10 × 0.18 |
| No. of reflections collected | 7947 |
| Θ(min., max.) [°] | 1.9, 28.1 |
| Observed data [$I > 2.0\ \sigma(I)$] | 2683 |
| Refinement | |
| *N*ref, *N*par | 3546, 208 |
| *R*, *wR*2[a], *S* | 0.0406, 0.1197, 1.10 |
| Residual densitiy (min., max.) [e/Å$^3$] | −0.38, 0.52 |

[a] $w = 1/[s^2(F_o^2) + (0.0640P)^2 + 0.0109P]$ where $P = (F_o^2 + 2F_c^2)/3$.

## Acknowledgments

The authors are grateful to the Council of Scientific and Industrial Research (Grant No. 01(1789)/02/EMR-II), New Delhi, India and the Spanish Government (Grant No. BQU2000/0791) for financial assistance. G. M. and T. H. L. thank the National Science Council, ROC for financial support (Grant Nos. NSC 90-2112-M-007-063 and NSC 91-2811-M-007-033). One of us (U. S. R.) thanks the UGC, for a fellowship.

[1] O. Kahn, *Molecular Magnetism*; John Wiley Sons, New York, **1993**.
[2] J. S. Miller, M. Drillon (Eds.), *Magnetism: Molecules to Materials IV*, Wiley-VCH, Weinheim, **2003**.
[3] S. R. Marder, J. E. Sohn, G. D. Stucky (Eds.), *Materials for Non-linear Optics: Chemical Perspectives*, ACS Symposium Ser., ACS, Washington, **1991**, p. 455.
[4] C. L. Bowes, G. A. Ogin, *Adv. Mater.* **1996**, *8*, 13.
[5] A. Hagfelot, M. Gratzel, *Acc. Chem. Res.* **2000**, *33*, 269.
[6] S. Chandrasekhar, *Liquid Crystals*, 2nd ed., Cambridge University Press, Cambridge, **1992**.
[7] Special issue on Focus on Self-assembly, *Acc. Chem. Res.* **1999**, *32*, no. 4.
[8] D. A. Buckingham, *Coord. Chem. Rev.* **1994**, *587*, 135.
[9] J. Ribas, A. Escuer, M. Monfort, R. Vicente, R. Cortés, L. Lezama, T. Rojo, *Coord. Chem. Rev.* **1999**, *193−195*, 1027.
[10] Z. E. Serna, L. Lezama, M. K. Urtiaga, M. Arriortua, M. G. B. Barandika, R. Cortes, T. Rojo, *Angew. Chem. Int. Ed.* **2000**, *39*, 344.
[11] G. S. Papaefstathiou, A. Escuer, C. P. Raptopoulou, A. Terzis, S. P. Perlepes, R. Vicente, *Eur. J. Inorg. Chem.* **2001**, 1567.
[12] M. A. S. Goher, J. Cano, Y. Journaux, M. A. M. Abu-Youssef, F. A. Mautner, A. Escuer, R. Vicente, *Chem. Eur. J.* **2000**, *6*, 778.
[13] C. S. Hong, S.-K. Son, Y. S. Lee, Y.-S. Kim, Y. Do, *Chem. Eur. J.* **2001**, *8*, 2239.
[14] S. Dalai, P. S. Mukherjee, T. Mallah, M. G. B. Drew, N. R. Chaudhuri, *Inorg. Chem. Commun.* **2002**, *5*, 472.
[15] Y. Xie, Q. Liu, H. Jiang, C. Du, X. Xu, M. Yu, Y. Zhu, *New J. Chem.* **2002**, *26*, 176.
[16] P. S. Mukherjee, T. Maji, A. Escuer, R. Vicente, J. Ribas, G. Rosair, F. A. Mautner, N. R. Chaudhuri, *Eur. J. Inorg. Chem.* **2002**, 943.
[17] H.-Y. Shen, W.-M. Bu, E. Q. Gao, D.-Z. Liao, Z.-H. Jiang, S. P. Yan, G.-L. Wang, *Inorg. Chem.* **2000**, *39*, 396.
[18] A. Escuer, R. Vicente, M. A. S. Goher, F. Mautner, *Inorg. Chem.* **1998**, *37*, 782.
[19] A. K. Sra, J. -P. Sutter, P. Guionneau, D. Chasseau, J. V. Yakhmi, O. Kahn, *Inorg. Chim. Acta* **2000**, 300−302, 778.
[20] P. Manikandan, R. Muthukumaran, K. R. Justin-Thomas, B. Varghese, G. V. R. Chandramouli, P. T. Manoharan, *Inorg. Chem.* **2001**, *40*, 2378 and refs. therein.
[21] L. Li, D. Liao, Z. Jiang, S. Yan, *Inorg. Chem.* **2002**, *41*, 1019.
[22] M. A. M. Abu-Youssef, A. Escuer, D. Gatteschi, M. A. S. Goher, F. A. Mautner, R. Vicente, *Inorg. Chem.* **1999**, *38*, 5716.
[23] M. A. M. Abu-Youssef, A. Escuer, M. A. S. Goher, F. A. Mautner, R. Vicente, *Eur. J. Inorg. Chem.* **1999**, 687.
[24] M. Villanueva, J. L. Mesa, M. K. Urtiaga, R. Cortes, L. Lezama, M. I. Arriortua, T. Rojo, *Eur. J. Inorg. Chem.* **2001**, 1581.
[25] E.-Q. Gao, S.-Q. Bai, Y.-F. Yue, Z.-M. Wang, C.-H. Yan, *Inorg. Chem.* **2003**, *42*, 3642.
[26] R. Cortes, M. Drillon, X. Solans, L. Lezama, T. Rojo, *Inorg. Chem.* **1997**, *36*, 677.
[27] L.-F. Tang, L. Zhang, L.-C. Li, P. Cheng, Z.-H. Wang, J.-T. Wang, *Inorg. Chem.* **1999**, *38*, 6326.
[28] M. Abu-Youssef, A. Escuer, M. A. S. Goher, F. A. Mautner, R. Vicente, *J. Chem. Soc., Dalton Trans.* **2000**, 413.
[29] H. Hou, Y. Wei, Y. Song, Z. Yinglin, Y. Zhu, L. Li, Y. Fan, *J. Mater. Chem.* **2002**, *12*, 838.
[30] J. L. Manson, A. M. Arif, J. S. Miller, *Chem. Commun.* **1999**, 1479.
[31] T. K. Misra, D. Das, C. Sinha, P. K. Ghosh, C. K. Pal, *Inorg. Chem.* **1998**, *37*, 1672.
[32] P. Byabartta, J. Dinda, P. K. Santra, C. Sinha, K. Panneerselvam, F.-L. Liao, T.-H. Lu, *J. Chem. Soc., Dalton Trans.* **2001**, 2825.
[33] P. Byabartta, Sk. Jasimuddin, B. K. Ghosh, C. Sinha, A. M. Z. Slawin, J. D. Woollins, *New J. Chem.* **2002**, *26*, 1415.
[34] D. Das, A. K. Das, C. Sinha, *Talanta* **1999**, *48*, 1013.

  

[35] Nakamoto, *Infrared and Raman Spectra of Inorganic and Coordination Compounds*, 5th ed., part B, John Wiley & Sons, Inc., New York, **1997**, pp. 124.
[36] A. B. P. Lever, *Inorganic Electronic Spectroscopy*, Elsevier Science Publishers B. V., Amsterdam, **1984**.
[37] A. Seal, S. Ray, *Acta Crystallogr. Sec C, Struct. Commun.* **1984**, *40*, 929.
[38] B. K. Ghosh, A. Mukhopadhyay, S. Goswami, S. Ray, A. Chakravorty, *Inorg. Chem.* **1984**, *23*, 4633.
[39] A. G. Orpen, L. Brammer, F. H. Allen, O. Kennard, D. G. Waston, R. Taylor, *J. Chem. Soc., Dalton Trans.* **1989**, SI.
[40] D. Das, PhD Thesis, Burdwan University, **1998**.
[41] G. R. Desiraju, in *The Crystals as a Supramolecular Entity* (Ed.: J. M. Lehn), John Wiley & Sons, Chichester, U. K., **1996**, vol 2.
[42] D. Braga, L. Maini, M. Polito, L. Scaccianoc, G. Cojazzi, F. Grepioni, *Coord. Chem. Rev.* **2001**, *216−217*, 225.
[43] U. S. Ray, G. Mostafa, T.-H. Lu, C. Sinha, *Cryst. Eng.* **2002**, *5*, 95.
[44] R. C. Carlin, *Magnetochemistry*, Springer Verlag, Berlin, **1986**, pp.148;.
[45] E. Ruiz, J. Cano, S. Alvarez, P. Alemany, *J. Am. Chem. Soc.* **1998**, *120*, 11122.
[46] M. Springbong (Ed.), *Density Functional Methods: Application in Chemistry and Material Science*, John Wiley & Sons, New-York, **1997**.
[47] S. R. Batten, P. Jensen, C. J. Kepert, M. Kurmoo, B. Moubaraki, K. S. Murray, D. J. Price, *J. Chem. Soc., Dalton Trans.* **1999**, 2987.
[48] A. Bencini, D. Gatteschi, *EPR of Exchange Coupled Systems*, Springer Verlag, Berlin, **1990**.
[49] B. J. Kennedy, K. S. Murray, *Inorg. Chem.* **1985**, *24*, 1552 and references cited therein.
[50] M. L. Kirk, M. S. Lah, C. Rattopoulou, D. P. Kessissoglou, W. E. Hatfield, V. L. Pecoraro, *Inorg. Chem.* **1991**, *30*, 3900.
[51] M. A. Martínez-Lorente, J. P. Tuchagues, V. Petroulas, J. M. Savariault, R. Poinsot, M. Drillon, *Inorg. Chem.* **1991**, *30*, 3589 and references cited therein.
[52] S. O. H. Gutschke, D. J. Price, A. K. Powell, P. T. Wood, *Angew. Chem. Int. Ed.* **1999**, *38*, 1088 and references cited therein.
[53] C.-M. Liu, Z. Yu, R.-G. Xiong, K. Liu, X.-Z. You, *Inorg. Chem. Commun.* **1999**, *2*, 31.
[54] A. Escuer, R. Vicente, M. A. S. Goher, F. Mautner, *Inorg. Chem.* **1997**, *36*, 3440.
[55] T. Moriya, *in Magnetism*, vol. 1 (Eds.: G. T. Rado, H. Suhl), Academic Press, London, **1963**, pp. 85.
[56] T. Moriya, *Phys. Rev.* **1960**, *117*, 635.
[57] A. K. Gregson, N. T. Moxon, *Inorg. Chem.* **1982**, *21*, 586.
[58] D. Armentano, G. De Munno, F. Lloret, A. V. Palii, M. Julve, *Inorg. Chem.* **2002**, *41*, 2007 and references cited therein.
[59] C. S. Hong, J.-E. Koo, S.-K. Son, Y. S. Lee, Y.-S. Kim, Y. Do, *Chem. Eur. J.* **2001**, *7*, 4243.
[60] C. S. Hong, Y. Do, *Angew. Chem. Int. Ed.* **1999**, *38*, 193.
[61] S. Han, J. L. Manson, J. Kim, J. S. Miller, *Inorg. Chem.* **2000**, *39*, 4184.
[62] S. R. Batten, P. Jensen, C. J. Kepert, M. Kurmoo, B. Moubaraki, K. S. Murray, D. J. Price, *J. Chem. Soc., Dalton Trans.* **1999**, 2987.
[63] G. M. Sheldrick, *SAINT*, version 5, Siemens Analytical X-ray Instrument Inc. Madison, WI, USA, **1995**.
[64] G. M. Sheldrick, *SHELXL-PLUS*, Siemens Analytical X-ray Instruments, Inc., Madison, Wisconsin, USA, **1990**; G. M. Sheldrick, *Acta Crystallogr., Sect. A* **1990**, *46*, 467.
[65] ORTEP-3, L. J. Farrugia, *J. Appl. Crystallogr.* **1997**, *30*, 565.
[66] A. L. Spek, *PLATON99, Molecular Geometry Program*, University of Utrecht, The Netherlands, **1999**.

Received June 26, 2003
Early View Article
Published Online November 6, 2003

  